

# Effect of Reionization on the Structure Formation in the Universe

Nickolay Y. Gnedin

CASA, University of Colorado, Boulder, CO 80309; e-mail: [gnedin@casa.colorado.edu](mailto:gnedin@casa.colorado.edu)

## ABSTRACT

I use the simulations of cosmological reionization to quantify the effect of the gas fraction suppression in the low density objects due to photoionization. I show that the Jeans mass does not match the characteristic mass scale below which the gas is efficiently expelled from the shallow potential wells, and which can be orders of magnitude lower than the Jeans mass. Instead, the filtering mass, that directly corresponds to the filtering scale over which the baryonic perturbations are smoothed in the linear theory, provides a remarkably good fit to the characteristic mass scale. I also derive the full shape of the probability distribution to find an object with a given gas mass among all the objects with the same total mass which depends exclusively on the filtering mass. The proposed probability distribution may be useful for semi-analytical modeling of structure formation in the universe.

*Subject headings:* cosmology: theory - cosmology: large-scale structure of universe - galaxies: formation - galaxies: intergalactic medium

## 1. Introduction

The effect of cosmological reionization on the formation and evolution of low mass objects has been under the scrutiny of theorists for a long time, ever since Ikeuchi (1986) and Rees (1986) independently pointed out that the increase in the temperature of the cosmic gas during reionization will suppress the formation of small galaxies with masses below the Jeans mass. Several attempts to quantify the effect of reionization on the low mass galaxies have been made since using semi-analytical calculations (Babul & Rees 1992; Efstathiou 1992), spherically symmetric modeling (Haiman, Thoul, & Loeb 1996; Thoul & Weinberg 1996), and three-dimensional cosmological hydrodynamic simulations (Quinn, Katz, & Efstathiou 1996; Weinberg, Hernquist, & Katz 1997; Navarro & Steinmetz 1997).

While confirming the general proposition that the reionization suppresses formation of the low mass galaxies, these studies sometimes contradict each other with, for example, Quinn et al. (1996) and Weinberg et al. (1997) claiming that galaxies with the circular velocities in excess of about 40 km/s are barely affected by the photoionization, whereas Thoul & Weinberg (1996) and Navarro & Steinmetz (1997) insist that objects with the circular velocities up to 80 km/s and even larger can be significantly affected by the heating of their gas content.

Table 1. Simulation Parameters

Run	$N$	Box size	Baryonic mass res.	Total mass res.	Spatial res.
A	$128^3$	$4h^{-1}$ Mpc	$10^{5.7} M_\odot$	$10^{6.6} M_\odot$	$1.0h^{-1}$ kpc
B	$128^3$	$2h^{-1}$ Mpc	$10^{4.8} M_\odot$	$10^{5.7} M_\odot$	$0.5h^{-1}$ kpc

This contradiction does not of course imply that some of the previous works are incorrect - different authors studied different cosmologies and different reionization histories of the universe, and a priori there is no reason to expect that in different cosmological models the effects of reionization would be the same.

Thus, it would be useful to attempt to quantify the effect of reionization on the formation and evolution of the low-mass objects in a more complete manner, relating the effective mass below which an object is a subject to the reionization feedback to the characteristic scales present at each given moment of time.

This paper attempts to accomplish precisely that based on the new simulations of the cosmological reionization. The simulations of a representative Cold Dark Matter cosmological model were performed with the “Softened Lagrangian Hydrodynamics” (SLH-P<sup>3</sup>M) code (Gnedin 1995, 1996; Gnedin & Bertschinger 1996) and fully described in Gnedin (2000). Table 1 lists two simulations used in this paper. Both simulations have sufficient mass resolution and the box size to resolve the relevant characteristic mass scales during reionization. Since both simulations have box sizes comparable to the nonlinear scale at the present time, they cannot be continued until  $z = 0$ . Rather, run A is stopped at  $z = 4$  and run B at  $z = 6.5$ .

The goal of this paper is to quantify the relationship between the total mass of an object  $M_t$  and its gas mass  $M_g$ . The advantage of using the simulations listed in Table 1 is that they have enough resolution (both in mass and space) to actually map the full two-dimensional distribution of objects in the  $M_t - M_g$  plane. But before this can be done, I need to discuss what characteristic mass scales are relevant for the evolution of the cosmic gas. This is particularly important because as the reader is reminded in the next section, the Jeans mass, initially proposed as the characteristic scale, is essentially irrelevant in the expanding universe.

## 2. Reminder: the Linear Theory

The effect of the reionization of the universe and the associated reheating of the cosmic gas on the evolution of linear perturbations was comprehensively discussed in Gnedin & Hui (1998). As they showed, the relationship between the linear overdensity of the dark matter  $\delta_d(t, k)$  and the

linear overdensity of the cosmic gas  $\delta_b(t, k)$  as a function of time and the comoving wavenumber  $k$ , in the limit of small  $k$ , can be written as

$$\frac{\delta_b(t, k)}{\delta_d(t, k)} = 1 - \frac{k^2}{k_F^2} + O(k^4), \quad (1)$$

where  $k_F$  is in general a function of time. They called the physical scale associated with the comoving wavenumber  $k_F$  the *filtering scale*, since it is the characteristic scale over which the baryonic perturbations are smoothed as compared to the dark matter.

The filtering scale is related to the Jeans scale  $k_J$ ,

$$k_J \equiv \frac{a}{c_S} \sqrt{4\pi G \bar{\rho}} \quad (2)$$

(here  $\bar{\rho}$  is the average total mass density of the universe,  $c_S$  is the sound speed, and  $a$  is the cosmological scale factor) by the following relation:

$$\frac{1}{k_F^2(t)} = \frac{1}{D_+(t)} \int_0^t dt' a^2(t') \frac{\dot{D}_+(t') + 2H(t')\dot{D}_+(t')}{k_J^2(t')} \int_{t'}^t \frac{dt''}{a^2(t'')}, \quad (3)$$

where  $D_+(t)$  is the linear growing mode in a given cosmology.

Inspection of equation (3) shows that the filtering scale *as a function of time* is related to the Jeans scale *as a function of time*, but at *a given moment in time* those two scales are unrelated and can be very different. Thus, given the Jeans scale at a specific moment in time, nothing can be said about the scale over which the baryonic perturbations are smoothed. It is only when the whole time evolution of the Jeans scale up to some moment in time is known, can the filtering scale at this moment be uniquely defined.<sup>1</sup>

The physical explanation of this result is very simple: the gas temperature (and thus the Jeans scale) can increase very quickly, but the gas density distribution can only change on the dynamical time scale, which is about the Hubble time for the linear perturbations. Thus, the effect of the increased pressure on the gas density distribution will be delayed and can only occur over the Hubble time.

While formally the filtering scale is only defined on large scales, as  $k \rightarrow 0$ , by an act of magic the following formula

$$\frac{\delta_b(t, k)}{\delta_d(t, k)} \approx e^{-k^2/k_F^2} \quad (4)$$

provides a remarkably accurate fit on all scales up to at least  $k = k_F$ , and is also very accurate when one needs to calculate the integrals over the baryonic power spectrum  $P_b(k) = \delta_b(t, k)^2$ . There is no physical reason why equation (4) should be a good fit to the full solution of the linear

---

<sup>1</sup>In general it is also true that the filtering scale is equal to the Jeans scale at some earlier moment in time.

theory equations, but it was extensively tested over a very large region of the parameter space of cosmological models and was always found to work well.

For a flat universe at high redshift  $z \gtrsim 2$ , the scale factor  $a$  is well approximated by the power-law in time,  $a \propto t^{2/3}$ , and the growing mode  $D_+$  is equal  $a$ . In this case equation (3) can be substantially simplified:

$$\frac{1}{k_F^2(a)} = \frac{3}{a} \int_0^a \frac{da'}{k_J^2(a')} \left[ 1 - \left( \frac{a'}{a} \right)^{1/2} \right]. \quad (5)$$

However, since my task is to compare the baryonic versus the total mass for small objects, it is convenient to switch from spatial to mass scales. In linear theory, of course, there exists a one-to-one relationship between the two. Thus, I can define the Jeans mass,

$$M_J \equiv \frac{4\pi}{3} \bar{\rho} \left( \frac{2\pi a}{k_J} \right)^3,$$

and the filtering mass,

$$M_F \equiv \frac{4\pi}{3} \bar{\rho} \left( \frac{2\pi a}{k_F} \right)^3,$$

as the mass enclosed in the sphere with the comoving radius equal to the corresponding spatial scale. The relationship between the two mass scales can be easily obtained from equation (5):

$$M_F^{2/3} = \frac{3}{a^3} \int_0^a da' a'^2 M_J^{2/3}(a') \left[ 1 - \left( \frac{a'}{a} \right)^{1/2} \right]. \quad (6)$$

### 3. Main Results

Figure 1 illustrates the relationship between the gas and the total mass of cosmological objects in the simulations.<sup>2</sup> Before the reionization ( $z = 15$ , light grey color) the gas mass is directly proportional to the total mass of all objects, and the coefficient of proportionality is the universal baryon fraction  $f_b \equiv \Omega_b/\Omega_0$ . In the simulation shown (run A) reionization occurs at  $z \approx 7$ , and at that redshift the effects of reheating start to appear. As time progresses, larger and larger mass objects are affected by the increase in the gas temperature.

The first quantity of interest is the average baryonic mass of all objects with the given total mass,  $\bar{M}_g(M_t)$ . This quantity would be useful for semi-analytical modeling since it can be directly plugged into the Press-Schechter approximation. Before reionization this function has a very simple form,  $\bar{M}_g = f_b M_t$ , but after reionization the small mass end of  $\bar{M}_g$  is suppressed. In order to obtain a practically useful result, I approximate the mean baryonic mass with the following fitting formula,

$$\bar{M}_g = \frac{f_b M_t}{(1 + M_C/M_t)^3},$$

---

<sup>2</sup>In all cases the stellar mass makes only a small correction to the total gas mass and is ignored.

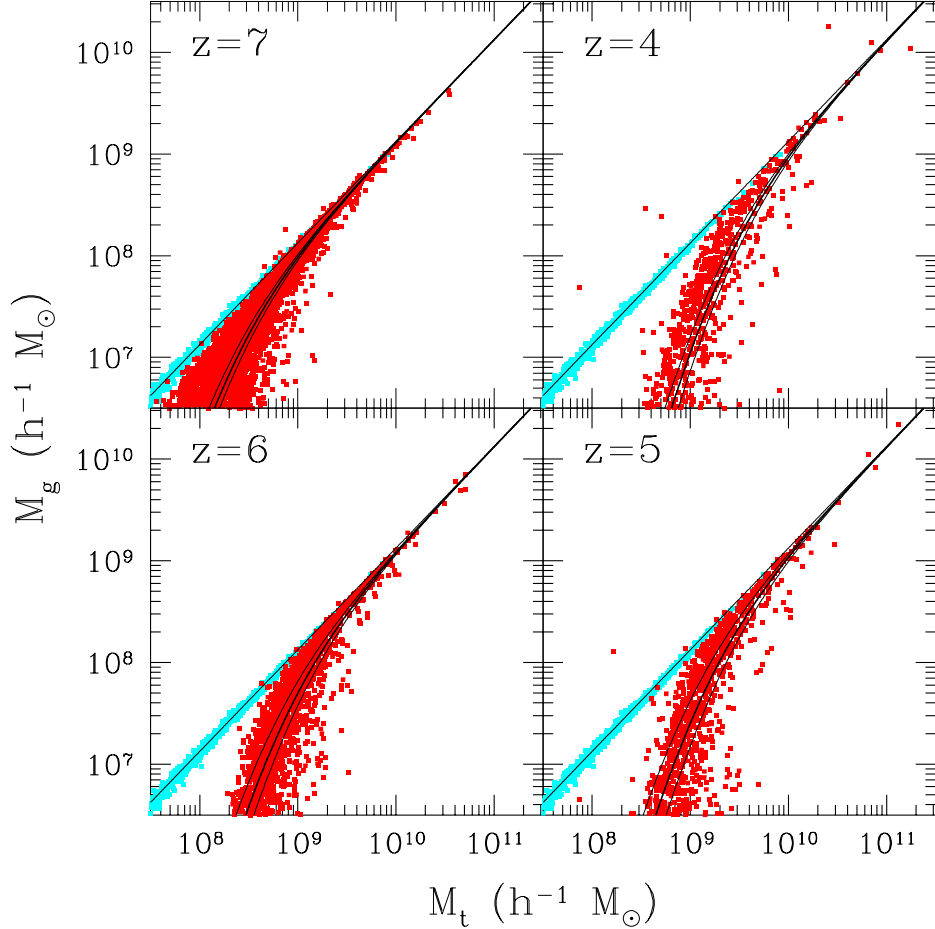


Fig. 1.— The gas versus the total mass for all objects from run A taken at four different redshifts (dark grey points). Also shown with the light grey color the gas versus total mass at  $z = 15$ . The straight line marks the position of the universal baryon fraction,  $M_g = (\Omega_b/\Omega_0)M_t$ , and three curved lines show the fit to the function  $\overline{M}_g(M_t)$  together with 95% confidence levels.

which depends on a single parameter - the characteristic mass  $M_C$ . The value of  $M_C$  and the corresponding errorbars are found by  $\chi^2$  minimization. The rationale for this particular choice of the fitting function is the following: it is clear from Fig. 1 that at small masses the mean baryonic mass goes as  $M_t^4$ . I have therefore tried the fitting formula of the following kind,

$$\overline{M}_g = \frac{f_b M_t}{[1 + (M_C/M_t)^\alpha]^{3/\alpha}},$$

and  $\alpha = 1$  gives the best values for the  $\chi^2$  test over the whole time evolution.<sup>3</sup>

<sup>3</sup>At selected moments in time an equally good fit can be obtained with different  $\alpha$ . For example, at  $z = 4$ ,  $\alpha = 2$  gives as good a fit as  $\alpha = 1$ , even if by eye it appears that  $\alpha = 2$  would be better than  $\alpha = 1$ . This is because Fig. 1 is shown on log-log scale, while  $\overline{M}_g$  is the average mass, and not the exponent of the average logarithm of mass.

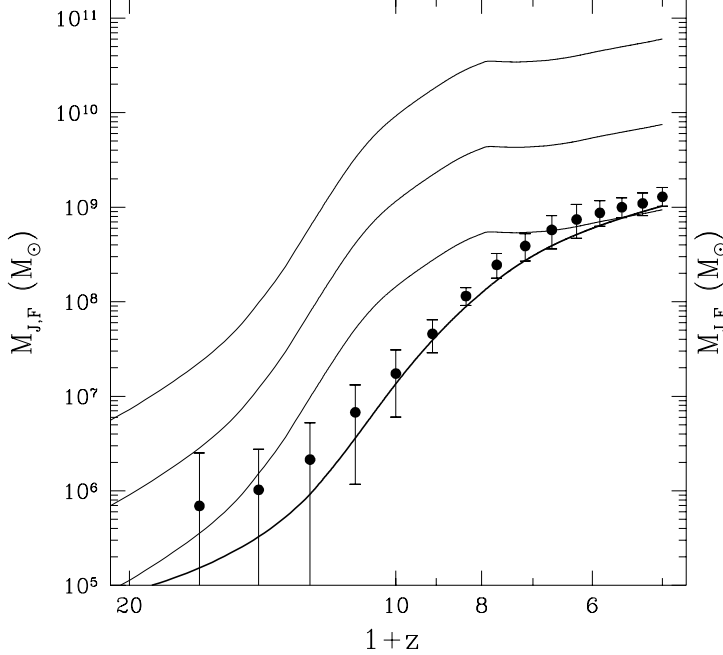


Fig. 2a

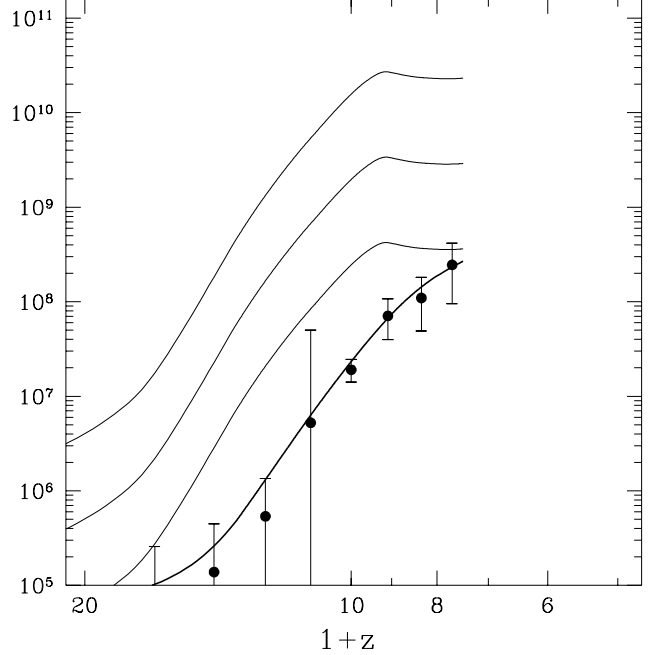


Fig. 2b

Fig. 2.— The evolution of various mass scales for two simulations: run A (a) and run B (b). The three thin lines show from the top down the Jeans mass ( $M_J$ ), the Jeans mass reduced by a factor of 8 ( $M_J/8$ ), and the Jeans mass reduced by a factor of 64 ( $M_J/64$ ). The bold line shows the filtering mass ( $M_F$ ), and the symbols with errorbars show the characteristic mass  $M_C$  as measured from the simulations.

Figure 2 now shows the evolution of the Jeans mass  $M_J$ , the filtering mass  $M_F$ , and the characteristic mass  $M_C$  for both simulations. One can immediately see that the filtering mass provides a good fit for the characteristic mass  $M_C$ , whereas the Jeans mass is much-much larger. Even if I decrease the Jeans mass by a factor of 8 (thus defining the Jeans mass as the mass within the sphere with the diameter, and not the radius, equal to the Jeans length), it is still way too high, and only if I further lower the Jeans mass by another factor of 8, it will give the correct characteristic mass at later times, but the overall shape is still wrong. Thus, I conclude that the filtering mass provides a very good approximation to the characteristic mass  $M_C$  which controls the relationship between the mean baryonic mass and the total mass of a cosmological object,

$$\overline{M}_g(M_t, t) \approx \frac{f_b M_t}{(1 + M_F(t)/M_t)^3}. \quad (7)$$

For most practical applications the knowledge of  $\overline{M}_g(M_t, t)$  may be sufficient, but the resolution of my simulations is also sufficient to approximately characterize the whole distribution function  $P(M_g, M_t)$ . Using the product rule of the probability theory, this distribution function can be written down as the product of the probability to find an object with the total mass  $M_t$

and the probability distribution of the gas masses for all objects with a given total mass,

$$P(M_g, M_t) = P(M_t)P(M_g|M_t).$$

The former probability depends on the cosmological model, whereas the latter may be conjectured to be independent of the specific model, and depend only on the characteristic mass scales present at this moment. The physical reason for this conjecture is simple: the number density of cosmological objects of a given mass depends on the cosmological model, but as long as this number density is not exceedingly high, different objects as virialized entities are independent of each other and the rest of the universe, and thus a probability for an object to lose a given fraction of its gas mass should not depend strongly on the abundance of other objects somewhere else in the universe.

The number of objects in the simulations is not high enough, of course, to accurately measure the probability distribution function  $P(M_g|M_t)$ , but it appears that for any  $M_t$  and at any given time this distribution is compatible with the lognormal distribution. Assuming, that it is indeed lognormal, I can write it down as follows:

$$P(M_g|M_t) = \frac{1}{\sigma\sqrt{2\pi}} \exp \left[ -\frac{1}{2\sigma^2} \left( \ln M_g - \ln \bar{M}_g + \sigma^2/2 \right)^2 \right], \quad (8)$$

where  $\sigma$  is the rms dispersion of the logarithm of the gas mass, and is a function of the total mass, as is  $\bar{M}_g$  (eq. [7]).

In order to come up with a closed form fitting formula, I approximate  $\sigma$  by the following power-law:

$$\sigma(M_t) = 2 \frac{M_C^*}{M_t},$$

where  $M_C^*$  is another characteristic mass, which is plotted in Figure 3 together with the Jeans mass and the filtering mass. Again, as one can see, the characteristic mass  $M_C^*$  is approximately equal to the filtering mass, so that the rms dispersion of the logarithm of gas mass at a given total mass is given by the following fit:

$$\sigma(M_t, t) \approx 2 \frac{M_F(t)}{M_t}, \quad (9)$$

Equations (7-9) give in a closed form the probability distribution function  $P(M_g|M_t, t)$  for any cosmological model and the reionization history (which are specified through the filtering mass  $M_F(t)$  as a function of time).

This work was partially supported by National Computational Science Alliance under grant AST-960015N and utilized the SGI/CRAY Origin 2000 array at the National Center for Supercomputing Applications (NCSA).

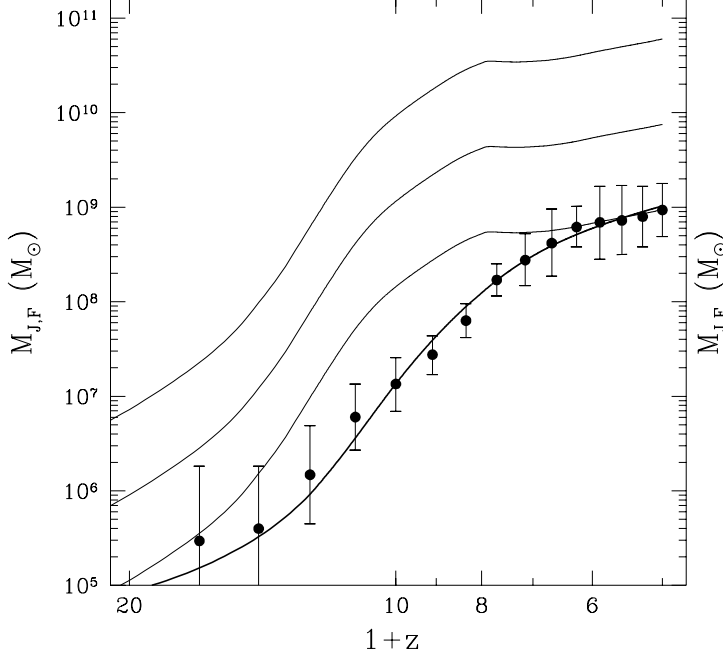


Fig. 3a

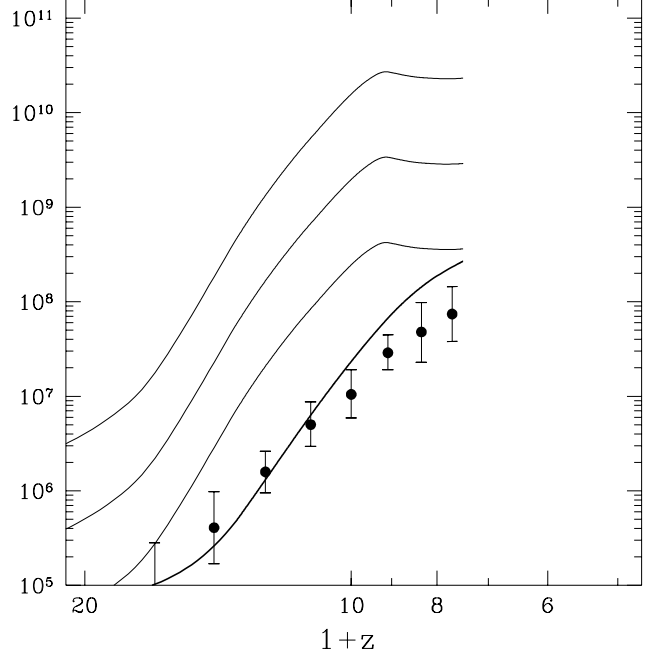


Fig. 3b

Fig. 3.— The same as Fig. 2, except that the symbols now show the characteristic mass  $M_C^*$  from the fitting formula for the rms dispersion  $\sigma$  of the lognormal distribution  $P(M_g|M_t)$  at a given  $M_t$ .

#### 4. Conclusions

Based on cosmological simulation of reionization, I showed that the Jeans mass does not control the mass scales over which the reionization suppresses the gas fraction in the low mass cosmological objects. Instead, the filtering mass, which directly corresponds to the length scale over which the baryonic perturbations are smoothed in the linear theory, provides a good fit to the characteristic mass scale.

The distribution of the gas fractions of all cosmological objects with the same total mass at any given moment during the evolution of the universe is approximately lognormal, is fully specified by the filtering mass at this moment, and is given by equations (7-9).

These equations, supplemented with the total-mass function of the cosmological objects, fully describe the full probability distribution to find an object with the given values of its gas and total mass. This probability distribution can be conveniently used in the semi-analytical modeling of the evolution of the low mass objects in the universe.

Admittedly, the simulations used in this paper consider only one cosmological model, but all cosmological models become matter-dominated at sufficiently high redshift, and follow the self-similar behavior. Thus, while the applicability of equations (7-9) for a wide range of cosmological models is not rigorously proven, the physical reasoning suggests that this is indeed

the case.

My simulations also do not cover all the possible reionization histories, but at least runs A and B have different reionization histories and different resolutions, which gives some credibility to the conjecture that equations (7-9) work for different reionization histories and are also free from numerical artifacts.

## REFERENCES

Babul, A., & Rees, M. J. 1992, MNRAS, 255, 346  
Efstathiou, G. 1992, MNRAS, 256, 43P  
Gnedin, N. Y. 1995, ApJS, 97, 231  
Gnedin, N. Y. 1996, ApJ, 456, 1  
Gnedin, N. Y. 2000, ApJ, in press (astro-ph/9909383)  
Gnedin, N. Y., & Bertschinger, E. 1996, ApJ, 470, 115  
Gnedin, N. Y., & Hui, L. 1998, MNRAS, 296, 44  
Haiman, Z., Thoul, A. A., & Loeb, A. 1996, ApJ, 464, 523  
Ikeuchi, S. 1986, Ap&SS, 118, 509  
Navarro, J., & Steinmetz, M. 1997, ApJ, 478, 13  
Quinn, T., Katz, N., & Efstathiou, G. 1996, ApJ, 278, 49P  
Rees, M. J. 1986, MNRAS, 218, 25P  
Thoul, A. A., & Weinberg, D. H. 1996, ApJ, 465, 608  
Weinberg, D. H., Hernquist, L., & Katz, N. 1997, ApJ, 477, 8